Correlated Multi-Technique Characterisation of Sulfur-Bearing Serpentine in Carbonaceous Chondrites

N. Topping[1], J. C. Bridges[1], L. J. Hicks[2] and T. Noguchi[3]

[1]School of Physics and Astronomy, University of Leicester, UK **(nt229@leicester.ac.uk)**, [2]School of Geology, Geography and the Environment, University of Leicester, UK, [3]Division of Earth and Planetary Sciences, Kyoto University, Kyoto, Japan

This presentation participates in OSPP — Outstanding Student & PhD candidate Presentation contest

Sharing is encouraged

1. Introduction:

Carbonaceous chondrites are the most primitive Solar System materials; they provide insights into early Solar System processes. In February 2020 the Winchcombe meteorite fell and was collected almost immediately, making it a near-pristine carbonaceous chondrite. JAXA's Hayabusa2 sample return mission successfully returned samples from C-type asteroid Ryugu, providing further pristine Solar System samples for study.

Phyllosilicates are the most abundant minerals across carbonaceous chondrites [1], with around 80% volume in both CM- and CI-type chondrites [2, 3, 4, 5]. These phyllosilicate minerals provide insights into processes in primitive parent bodies of the early Solar System. It is widely agreed that CM- and CI-type carbonaceous chondrites underwent aqueous alteration on their parent bodies, resulting in phyllosilicate-rich matrices where the dominant mineral phase is serpentine-like material. Serpentine is a sheet silicate, with structure that follows a repeating unit of tetrahedral and octahedral (T-O) site occupancy layers (1:1) and a [0 0 1] basal plane spacing of 0.70 nm [6].

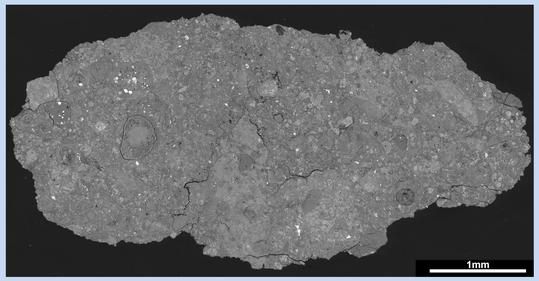

Figure 1: Back-scattered electron (BSE) SEM image taken of thin section sample Winchcombe P30543 using the FEI Quanta 650 FEG SEM at Uni. of Leicester Advanced Microscopy Facility, UK.

2. Scientific Context:

Despite its importance for understanding the origin and evolution of our Solar System, the structure of serpentine is not well-known. Previous studies have been conducted on phyllosilicate structure in carbonaceous chondrites, however the serpentine-like phases are often grouped as 'poorly characterised phases' (PCPs) in the literature [1].

The presence of sulfur in these serpentine-like minerals and its effect on crystal lattice structure has not been studied in detail. Sulfur is significant in planetary mineralogy and cosmochemistry as it is a good indicator of redox conditions on the parent bodies. We are investigating how the presence of sulfur (up to 9-10 wt% SO_3) in serpentine phyllosilicate regions effects basal lattice spacing measurements in CM- and CI-type chondritic and related asteroidal material.

3. Samples and Methods:

Samples: Four specimens are being studied and all are TEM wafers. *CM-type*: Winchcombe and Aguas Zarcas. *CI-type*: Ivuna and Ryugu (samples A0058-C2001-08, A0104-00200502 and A0104-01700602 from Hayabusa2).

A multi-technique approach is being adopted to study these samples, using the JEOL ARM200CF and JEOL ARM300CF electron microscopes at E01 and E02, respectively, at the ePSIC facility at Diamond Light Source (DLS), Harwell, UK. EDS compositional data is collected using the E01 microscope, whilst HRTEM and HAADF imaging data is collected at E02. Using E02 we are also applying a new 4D-STEM nano-diffraction technique which should correlate with our other HRTEM measurements. Fe-K XANES analyses on Winchcombe and Ryugu [7] have been carried out using the I18 microprobe and I14 hard x-ray nanoprobe respectively, also at DLS, to constrain $Fe^{3+}/\Sigma Fe$. By combining these techniques, we aim to better understand the physical and chemical structure of serpentine-like minerals in carbonaceous chondrites. This multi-technique approach could then be applied to future sample return missions (Mars2020, OSIRIS-REx) and meteorite falls.

4. Results and Discussion:

Using EDS, we have been able to identify S-poor and S-bearing regions across all four samples. We have taken S-bearing to be anything with >1 wt% SO_3. The error is ~±3.5 wt%, and the EDS is currently analysed on an Al- free basis pending quantification checks.

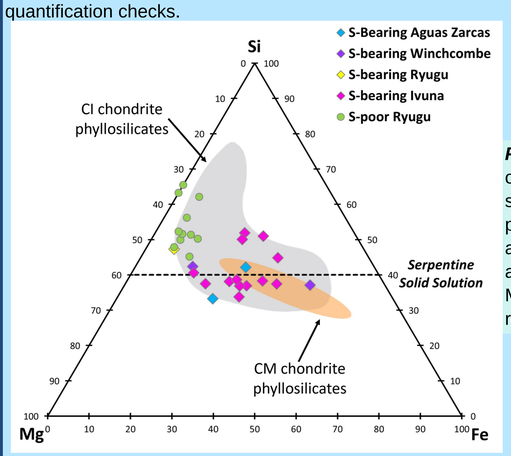

Figure 2: Ternary diagram of EDS results from data collected on E01 microscope at ePSIC, DLS. Results from all four samples are shown on the Si-Mg-Fe system. Results are plotted in atomic%. The data is plotted with a shaded grey area for CI chondrite phyllosilicates and an orange shaded area for CM chondrite phyllosilicates, based on results from Morlock et al (2006) [8] and Zolensky et al (1993) [9], respectively.

Ryugu results appear to display a high percentage of Si content compared to what is expected, likely due to the exclusion of the Al. Another reason is due to overlap with some FeS grains in the EDS regions; here Fe appears to be constrained to the sulfide grains (based on elemental mapping), thus was removed from the final quantification. When comparing the Ryugu S-poor data points to other Ryugu phyllosilicate analyses (see figure 2 in [4]), they lie within the expected area on the ternary plot. Most Ryugu measurements detected no sulfur, which is expected as there is high FeS content in this sample.

For HRTEM analyses, five measurements were taken per HRTEM image to determine d_{001}-spacing values. These TEM analyses show lattice spacings that are characteristic of the 1:1 layered T-O serpentine-group phyllosilicates. For the CMs, d-spacings of 0.60-0.70 nm (±0.03 nm) are likely the S-bearing regions, whilst 0.70-0.74 nm (±0.03 nm) are S-poor regions. Similarly for the CIs, 0.63-0.70 nm (±0.02 nm) spacings are for S-bearing regions and 0.70-0.76 nm (±0.02 nm) for S-poor.

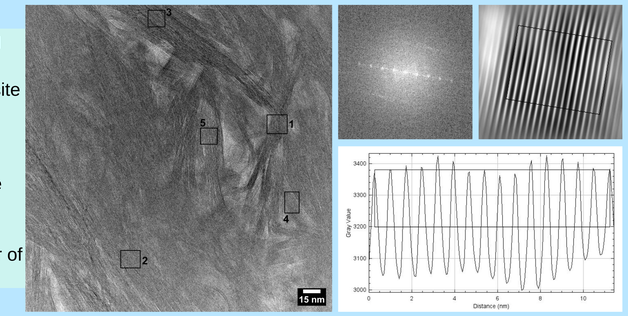

Figure 3: Winchcombe HRTEM. *Left:* HRTEM image annotated with sites where lattice measurements were taken. Top right: FFT of site 1, contrast and brightness adjusted, and the inverse of the FFT, with the area measured outlined. *Bottom right:* Profile plot of selected area. A box is drawn across the peaks and the distance between end peak centres is measured. The d-spacing is calculated by dividing the measured distance by the number of peaks.

The nano-diffraction work is currently in progress, however preliminary results from these analyses show it is a useful tool for identifying different regions responsible for different diffraction patterns across a sample. Figure 4 is an example of the output from nano-diffraction analyses.

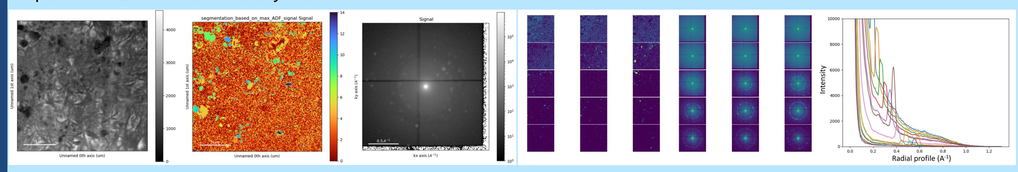

Figure 4: T1_Ryugu_P035_GR25_B.

Left-Right: Dark-field image of nano-diffraction region; heat-map of the region where different colours represent the different areas responsible for different diffraction patterns; the diffraction pattern for the whole region; analysis area segmented into 15 regions shown with their corresponding diffraction patterns; and all 15 radial profiles of each diffraction pattern are shown plotted together.

5. Conclusions:

We can conclude that S-bearing regions of serpentine-like minerals have been identified using EDS, and that in these areas the presence of sulfur appears to reduce basal lattice spacings compared to the expected value of 0.70 nm [6].

From EDS analyses and figure 2, the addition of sulfur alters the stoichiometry of serpentine-like minerals. The Si content seems to reduce, which could indicate that S is present in the tetrahedral sites of the T-O layers.

Differences in lattice spacing ranges between the CMs and the CIs are likely due to the redox state of S. In Winchcombe and Aguas Zarcas, more of the S seems to be in the serpentine structure, whereas in Ryugu and other CI-types the S appears in the reduced form as FeS grains, with lower S content in the serpentine regions. Possible reasons include further studies into the valency of the S ions, the bonding environment within serpentine T-O layers, and the location of S in either tetra- or octahedral sites.

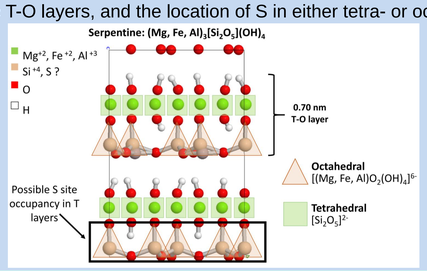

Figure 5: Serpentine structure (packed unit cell, courtesy of mindat.org) with repeating T-O layers. Initial EDS results suggest it is possible that the S is located in the tetrahedral sites (also suggested in Debret et al (2017) [10]).

6. Future Work:

We will continue with our work using E01 and E02 facilities at ePSIC, extending EDS analyses for the CM chondrites; collecting more Winchcombe and Aguas Zarcas data and analysing new samples such as Murchison and Tagish Lake. Further HRTEM measurements on the additional samples will be taken at E02. Similarly, the EDS and HRTEM datasets for the CI chondrites can be extended by analysing specimens such as Orgueil. At ePSIC we will also continue working on the application of 4D-STEM nano-diffraction as a complementary technique to HRTEM lattice measurements.

We have planned for beam-time at DLS on the I18 microprobe beamline for S-K edge XANES and XAFS on S-bearing serpentine-like minerals, in order to determine sulfur site occupancy and S-compound bond lengths. It will be a comprehensive XAS investigation of S-bearing mineral phases such as sulfides, serpentine and tochilinite in CM and CI chondrites. The high spatial resolution of the I18 beamline (2 x 2 µm) [11] will help avoid mixing of the signals from FeS grains and silicate regions. Initial work will begin with Winchcombe, Ivuna, Murchison and Tagish Lake, to be followed with analyses of Ryugu and Bennu (OSIRIS-REx) on I14 at DLS. The preliminary I18 chondrite analyses will form the basis for understanding S-redox and mineralogy in primitive asteroids (Ryugu, Bennu).

7. Acknowledgements:

We thank Diamond Light Source for access and support in use of the electron Physical Science Imaging Centre (instruments E01 and E02, proposals MG30752 and MG31953) that contributed to the results presented here. Particular thanks to Dr Christopher Allen for his help.

8. References:

[1] Brearley A. & Jones R. (1998), ed. Papike, J. J., Chondritic Meteorites in *Planetary Materials.*

[2] King A.J. et al (2022), *Science Advances, 8(46).*

[3] Garvie L, (2021), *American Mineralogist, 106(12),* 1900-1916.

[4] Ito M. et al (2022), *Nature Astronomy, 6,* 1163-1171.

[5] King A.J. et al (2015), *Geochimica et Cosmochimica Acta, 165,* 148-160.

[6] Hicks L.J. et al (2014), *Geochimica et Cosmochimica Acta, 136,* 194-210.

[7] Noguchi T. et al (2023), *Nat Astron, 7,* 170-181.

[8] Morlock A. et al (2006), *Geochimica et Cosmochimica Acta, 70,* 5371-5394.

[9] Zolensky M. et al (1993), *Geochimica et Cosmochimica Acta, 57,* 3123-3148.

[10] Debret B. et al (2017), *Earth and Planetary Science Letters, 466,* 1-11

[11] DLS, https://www.diamond.ac.uk/Instruments/Spectroscopy/I18/Specification.html